Debris Disk
Radiative Transfer Simulation Tool (DDS)

S. Wolf [a,b], L. A. Hillenbrand [b],

[a] *Max Planck Institute for Astronomy, Königstuhl 17, 69117 Heidelberg, Germany, swolf@mpia.de*

[b] *California Institute of Technology, 1201 E California Blvd, Mail Code 105-24, Pasadena CA 91125, USA*

Abstract

A WWW interface for the simulation of spectral energy distributions of optically thin dust configurations with an embedded radiative source is presented. The density distribution, radiative source, and dust parameters can be either selected from an internal database or be defined by the user. This tool is optimized for studying circumstellar debris disks where large grains ($a_{\rm grain} \gg 1\mu$m) are expected to determine the (sub)millimeter dust reemission spectral energy distribution. The tool is available at `http://aida28.mpia-hd.mpg.de/~swolf/dds`.

PACS:
94.10.Gb - Absorption and scattering of radiation
97.21.+a - Pre-main sequence objects, young stellar objects and protostars
97.82.+k - Extrasolar planetary systems

Key words:
Radiative transfer, dust, absorption, scattering, debris disk – astrophysics

---

1 Introduction

The *Debris Disk Radiative Transfer Simulation Tool* (DDS) was developed with the aim to provide a flexible tool for the simulation of spectral energy distributions (SEDs) of circumstellar debris disks. Debris disks are solar system sized dust disks with micron-sized grains produced as by-products of collisions between asteroid-like bodies being left over from the planet formation process. In the case of our solar system, the debris of Jupiter-family short-period comets and colliding asteroids represents the dominant sources of zodiacal dust located between Mars and Jupiter. A second belt of dust is located beyond the orbit of Neptune (see, e.g., Dermott et al. 1992, Liou, Dermott, & Xu 1995). Besides the solar system, optical to mid-infrared images of β Pic (see, e.g., Kalas & Jewitt 1995; Weinberger, Becklin, & Zuckerman 2003) and submillimeter images of Vega, Fomalhaut, and ϵ Eri (Holland et al. 1998; Greaves et al. 1998) have revealed spatially resolved debris disks which were first inferred from observations of infrared flux excesses above photospheric values with IRAS. The mass of small grains in debris disks and therefore the thermal dust reemission from these disks is expected to be much smaller than in case of T Tauri disks. For this reason, only a very limited sample of observations exists so far. However, because of the high sensitivity of the mid-infrared detectors aboard the *Spitzer Space Telescope* followed by the *Stratospheric Observatory for Infrared Astronomy* (*SOFIA*), a substantial increase in the total number and in the specific information about debris disks is expected (c.f. Meyer 2001).

The range of applications of the DDS, however, extends far beyond debris disks (or similar, e.g. disk-like structures) allowing to derive the reemission and scattered light SED for *any* three-dimensional optically thin dust distribution: In the optically thin limit only the radial distance r between each individual grain of a dust distribution determines this grain's contribution to the net SED. Thus, any arbitrarily shaped configuration described, e.g. by a three-dimensional denisty distribution $\rho(x, y, z)$ can be reduced to an equivalent one-dimensional distribution $\rho(r)$ in respect of its resulting thermal reemission and scattered light SED (r is the radial distance from the central star / heating source). The DDS is therefore best characterized as a *tool for the simulation of scattered light and thermal reemission in arbitrary optically thin dust distributions with spherical, homogeneous grains where the dust parameters (optical properties, sublimation temperature, grain size) and SED of the illuminating/heating radiative source can be arbitrarily defined.*

2 The method

The solution of the radiative transfer problem implemented in the DDS is based on three assumptions:

(1) The dust configuration is optically thin along any line of sight for both the stellar as well as for the reemission radiation from the dust,
(2) The dust grains are compact spheres with a homogeneous chemical structure, and
(3) The dust grains are large enough to be in thermal equilibrium with the ambient radiation field.

In the optically thin limit, each dust grain is heated by direct stellar radiation only. Thus, the dust grain temperature is a function of the optical parameters of the grains, the incident stellar radiation, and the distance r from the star. In this case the radiative transfer equation has a simple solution which allows one to derive the distance from the star at which the dust has a certain temperature. Let

$$L_{\lambda,\mathrm{s}} = 4\pi R_{\mathrm{s}}^2 \pi B_\lambda(T_{\mathrm{s}}) \tag{1}$$

be the monochromatic luminosity of the star (radius R_{s}, effective temperature T_{s}) at wavelength λ and

$$L_{\lambda,\mathrm{g}}^{\mathrm{abs}} = L_{\mathrm{s}} Q_\lambda^{\mathrm{abs}} \frac{\pi a^2}{4\pi r^2} \qquad \text{and} \tag{2}$$

$$L_{\lambda,\mathrm{g}}^{\mathrm{emi}} = 4\pi a^2 Q_\lambda^{\mathrm{abs}} \pi B_\lambda(T_{\mathrm{g}}) \tag{3}$$

be the absorbed and reemitted luminosity of a dust grain with radius a and resulting temperature T_{g} at the (unknown) radial distance r from the star. Using the constraint of energy conservation

$$\int_0^\infty L_{\lambda,\mathrm{g}}^{\mathrm{emi}} d\lambda = \int_0^\infty L_{\lambda,\mathrm{g}}^{\mathrm{abs}} d\lambda \tag{4}$$

one derives the distance of the grain from the star as

$$r(T_{\mathrm{g}}) = \frac{R_{\mathrm{s}}}{2} \sqrt{\frac{\int_0^\infty d\lambda Q_\lambda^{\mathrm{abs}}(a) B_\lambda(T_{\mathrm{s}})}{\int_0^\infty d\lambda Q_\lambda^{\mathrm{abs}}(a) B_\lambda(T_{\mathrm{g}})}}. \tag{5}$$

If the dust sublimation temperature is known, Eq. 5 also allows one to estimate the sublimation radius r_{sub} for each dust component in the shell (characterized by the grain radius and chemical composition). The flux of the light scattered by a single dust grain amounts to

$$L_{\lambda,\mathrm{g}}^{\mathrm{sca}} = L_{\lambda,\mathrm{s}} A Q_{\lambda}^{\mathrm{sca}} \left(\frac{a}{2r}\right)^2 , \tag{6}$$

where A is the dust grain's albedo. The net spectral energy distribution results from a simple summation of the reemitted and scattered light contributions from all grains.

The interaction of the stellar radiation field with the dust grains - characterized by the efficiency factors $Q_{\lambda}^{\mathrm{abs}}$ and $Q_{\lambda}^{\mathrm{sca}}$ (and thus the albedo A) - is described by Mie scattering theory in the DDS. The Mie scattering function is calculated using the numerical solution for the estimation of the Mie scattering coefficients published by Wolf & Voshchinnikov (2004; see also Voshchinnikov 2004), which achieves accurate results both in the small as well as in the – arbitrarily – large size parameter regime.

3 Numerical Implementation

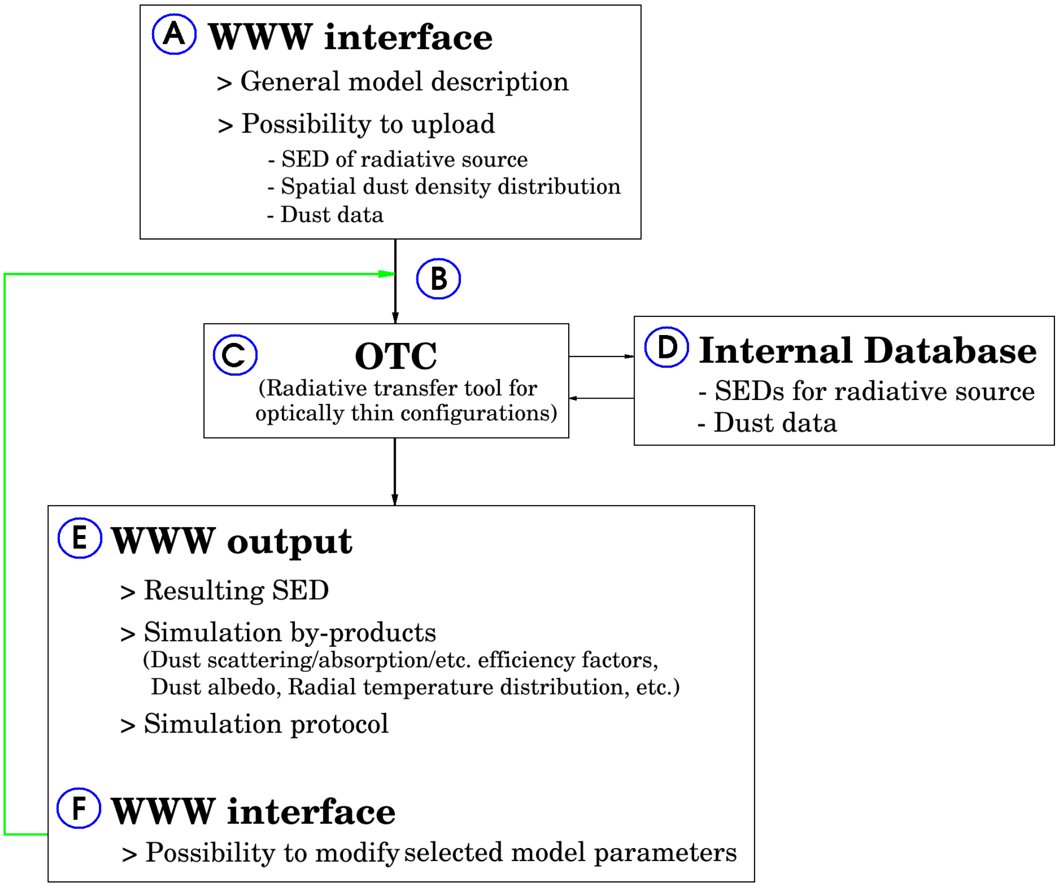

Fig. 1. DDS data flowchart.

In this section the general scheme and main features of the DDS are described. For this reason a simplified chart symbolizing the data flow is given in Fig. 1. The single units, symbolized by letters `A - F` in Fig. 1, solve following tasks:

A:
WWW interface: Model setup (see Fig. 2).
Each debris disk model to be investigated with the DDS (or dust configuration model in general) is defined by

(1) The SED of the radiative source which is given
  (a) analytically as a blackbody radiator characterized by its temperature and total luminosity,
  (b) by an internally defined SED (e.g. the solar SED), or
  (c) by the user; the format of the upload-files containing the SED is given in Sect. A.1.

(2) The inner and outer radius of the disk. If an uploaded density distribution (see 3. below) is considered, the inner and outer radius defined in that file are used. If a fixed inner radius is chosen which turns out to be within the sublimation region of a particular dust species (defined by its grain size and chemical composition), the sublimation radius is used for this dust species instead.
(3) The disk density distribution, which is either
    (a) described analytically (by the radial density profile and opening angle of the disk), or
    (b) provided by the user in form of an upload-file (see Sect. A.2 for the file format).
(4) The disk mass, i.e. the total mass of all dust grains,
(5) The dust grain size distribution given by the minimum and maximum grain size and an exponent that describes the slope of the distribution,
(6) The relative abundances of the chemical components. Beside a menu of predefined chemical components the possibility to upload further components is provided (see Sect. A.3 for the file structure). These abundances represent either relative mass densities per volume element or relative number densities of dust grains.
(7) The specification of the observable SED to be simulated (wavelength distribution).

B:
The handing over of the input parameters and file upload are managed by PERL and CGI scripts. The input parameters are stored in a file which is processed by unit C (see below).

C:
The OTC is a radiative transfer tool optimized for <u>o</u>ptically <u>t</u>hin <u>c</u>onfigurations. It is written in Fortran 90 and solves following tasks:

(1) Evaluation of the input data:
    (a) Data type verification for each input value,
    (b) Test of the model integrity, and
    (c) Test of specific upper / lower limits of input parameter values.

(2) Calculation of the SED:
    (a) Definition of the wavelength range and wavelengths at which the dust absorption (and based on this the dust temperature distribution) shall be calculated. In case of a blackbody radiative source, this wavelength range is derived under consideration of the blackbody temperature. A fixed number of wavelengths ($\sim$ 500) is then distributed logarithmically equidistantly within this range. In case of uploaded SEDs for the radiative source or the choice of one of the SEDs from the internal database (see unit D below), the given

wavelengths / wavelength range are used.

(b) Calculation of the dust absorption efficiencies at the wavelengths of stellar emission (for dust absorption only) and the user-defined observing wavelengths for each grain size (a_i) and chemical composition (ξ_j).

(c) Calculation of the radial distances $r(T, a_i, \xi_j)$ of the dust grains to the heating source that correspond to predefined temperatures (see Eq. 5; $2.73\text{K} \leq T \leq$ sublimation temperature).

(d) If the density distribution is provided on a grid, the array $r(T, a, \xi)$ is interpolated in order to provide the identical radial spatial resolution as the uploaded density distribution.

(e) If required: Calculation of the scattering efficiency of the dust grains at the observing wavelengths.

(f) Calculation of the relative net contribution of each individual dust species outside the corresponding sublimation radius.

(g) Summation over the net contributions and normalization of the total flux based on the total dust mass in the model.

(3) Creation of all output files:

(a) for the user: final results (resulting SED, radial temperature distribution, etc.),

(b) internally: intermediate results, such as the relative contributions of each dust species to the net SED; these files are required in unit F (see below).

D:

A selection of astrophysically relevant dust data and SEDs of radiative sources [1] is compiled in an internal database. The optical data of following dust species have been included so far:

(1) Silicates, oxides, and carbon configurations published by Dorschner et al. 1995 and Jäger et al. 1998 made available at `http://www.astro.uni-jena.de/Laboratory/Database/odata.html` (Henning et al. 1999), and

(2) "Astronomical silicate" and graphite published by Weingartner & Draine (2001).

Detailed references are given in unit A.

E:

Presentation of all results on a WWW page (see Fig. 1 for an example).

[1] So far, only the solar SED is included (from measurements published by Labs & Neckel 1968). Further SEDs are planned to be included according to the response of the user community.

F:
The WWW page with the results also allows to modify selected model parameters, such as

(1) Disk mass,
(2) Grain size distribution slope,
(3) Relative abundances of individual chemical components, and
(4) Distance.

Based on the intermediate results stored in unit C (step 3), a simple new weighting of the relative flux contributions from the individual grains species allows a quick calculation of the SED of the modified model.

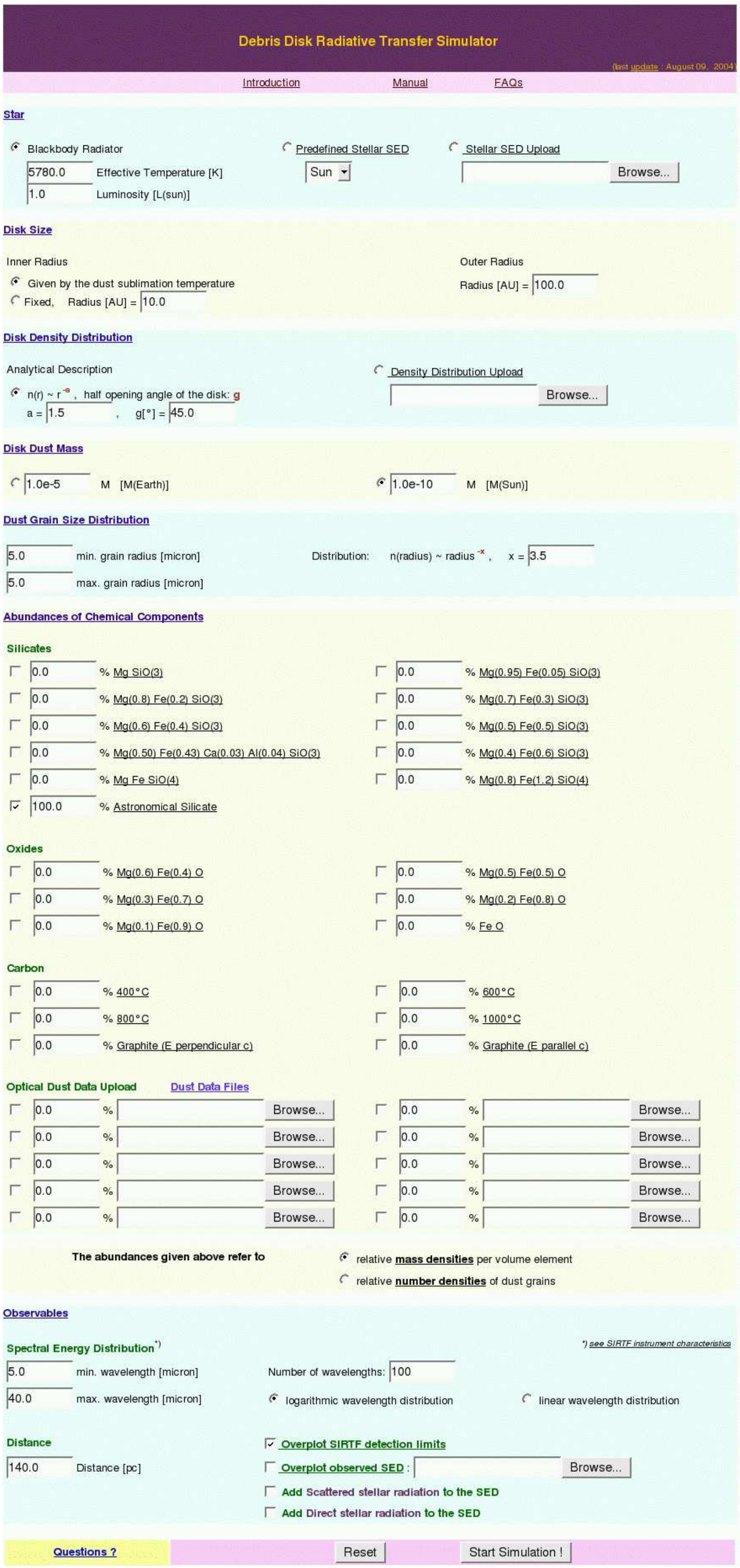

Fig. 2. DDS: Input mask.

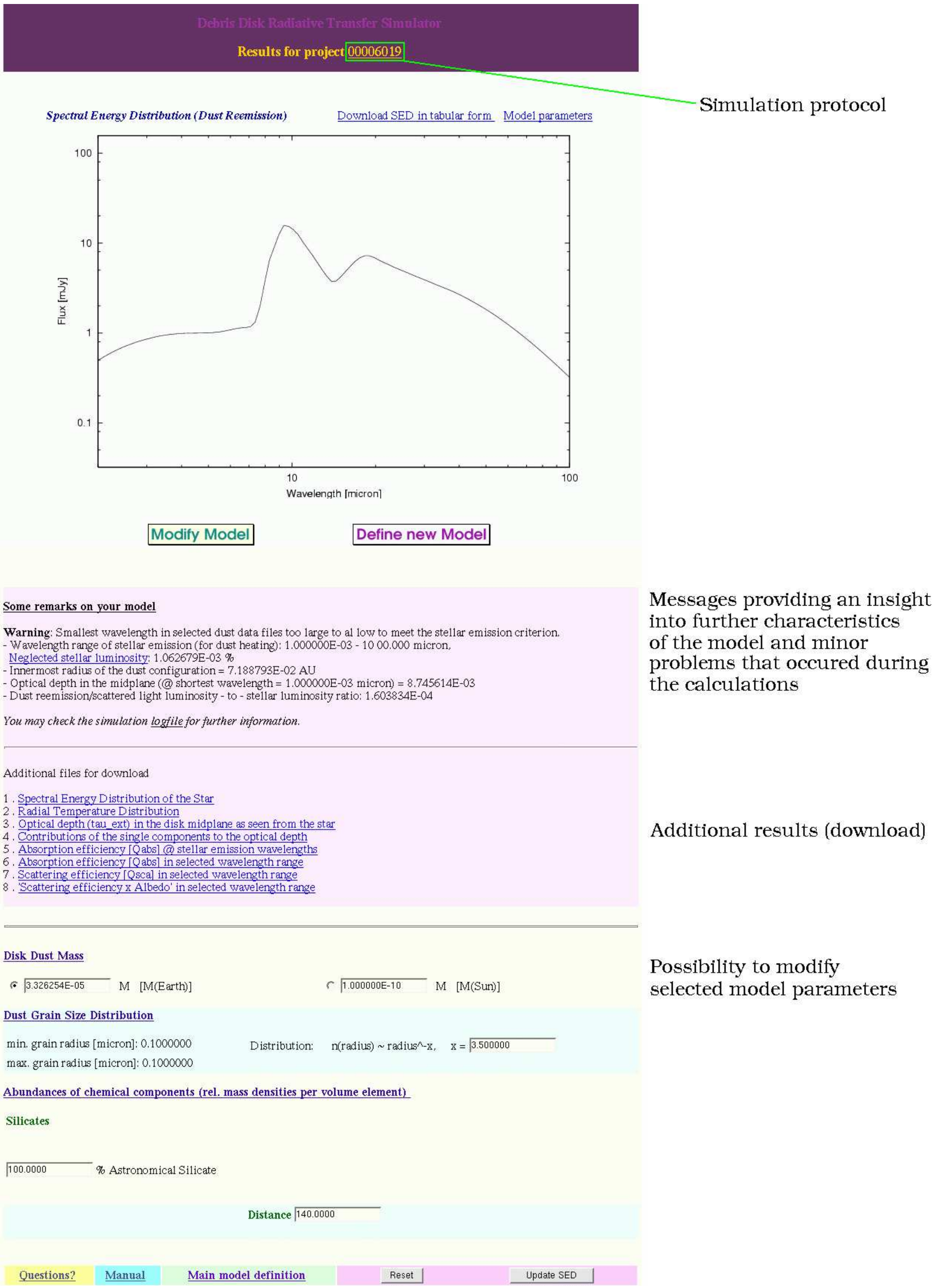

Fig. 3. DDS: Example output.

4 Performance of the code

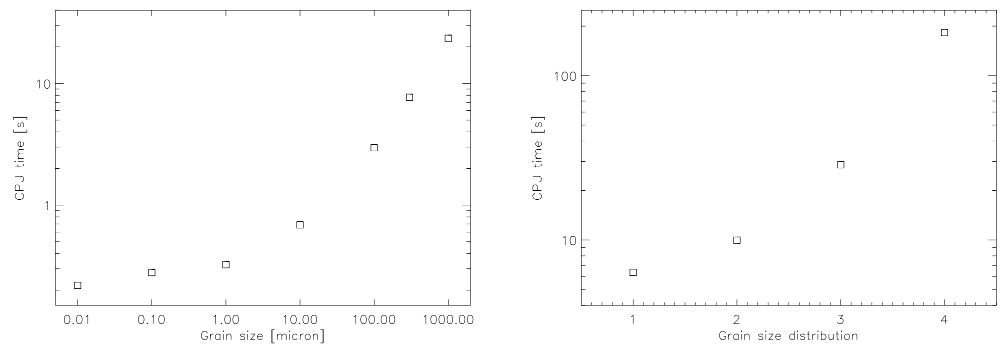

Fig. 4. Performance of OTC/DDS: Run-time of the code as a function of grain size: [**A**] Single grain sizes; [**B**] Grain size distributions (1: 0.01-1μm, 2: 0.1-10μm, 3: 1-100μm, 4: 10-1000μm). For this test the dust reemission has been calculated for 100 wavelengths linearly distributed in the range 10-100μm. Otherwise, default settings have been used, such as 500 wavelengths to simulate the stellar emission. The CPU times have been estimated on an Intel(R) XEON(TM) 2.20 GHz processor using the Intel Fortran 90 compiler for Linux.

The runtime of the code is mainly determined by the grain size (distribution) and number of wavelengths (a) at which absorption of the stellar light is modelled (typically $\sim$ 500) and (b) at which the observable SED has to be calculated (defined by the user). The reason for this behaviour is that the dust grain parameters (efficiency factors, albedo - see Sect. 2) are calculated in each individual simulation in order to provide maximum flexibility in the choice of the grain size distribution. For a fixed model setup with a single grain size (defined by minimum grain size = maximum grain size) the run-time of the code as a function of grain size is shown in Fig. 4[A]. For selected grain size distributions (defined by: minimum grain size $<$ maximum grain size) the run-times are shown in Fig. 4[B]. In the latter case, 32 individual grain sizes logarithmically equidistantly distributed between the minimum and maximum grain size, are considered for each chemical component.

The OTC/DDS has been tested by comparing its results (radial temperature distribution, reemission and scattered light SED) with those obtained with the radiative transfer code MC3D (Wolf 2003). The results agree within the numerical accuracy, i.e. both codes produce practically the same results.

5 Acknowledgments

S.W. was supported through the German Research Foundation (Emmy Noether Research Program WO 857/2-1), through the NASA grant NAG5-11645, and through the SIRTF (Spitzer Space Telescope) legacy science program through an award issued by JPL/CIT under NASA contract 1407. The program *gnuplot* [Copyright (C) 1986-1993, 1998; Th. Williams & C. Kelley] is implemented in the DDS. I wish to thank A. Moro-Martín and J. Rodmann for their help to test the DDS and all members of the FEPS team for valuable discussions.

A Input file formats

The SED of the illuminating and heating source, the dust density distribution, and additional dust species can be uploaded in form of ASCII files. These files must have tabular structures which are described in Sect. A.1-A.4. The file structures are described in an online help webpage, which is connected via links to each of the individual upload sections. Since the particular file structure of some of the input files may be changed over time, only the links to the help pages are given in those cases.

A.1 Stellar SED

The file structure for stellar SEDs is identical to internally predefined stellar SEDs (see there for examples). It is documented at
http://aida28.mpia-hd.mpg.de/~swolf/dds/dds-manual.html#stellar_sed_upload.

A.2 Density Distribution

If $n_0(r, \theta, \phi)$ is the arbitrary (optically thin) density distribution, the radial density distribution $n(r)$ required for the simulation of the SED can be derived as follows (simply averaging):

$$n(r) = \frac{1}{4\pi} \int_0^{2\pi} \int_0^{\pi} n_0(r, \theta, \phi) \sin\theta \, d\theta \, d\phi. \tag{A.1}$$

The structure of the file for density upload is documented in Tab. A.1.

# Header with remarks etc. (optional) # ...	
Number radial grid points *[integer]*	
Radial distance r from the source [AU] *[float]* ...	Corresponding relative dust grain number density $n(r)$ *[float]* ...

Table A.1
File structure required for dust density distributions.

When providing the set of pairs $(r, n(r))$, the following guidelines should be considered:

(1) The distance between two subsequent radial points should decrease towards the heating source in order to allow the code (OTC) to resolve the increasing radial temperature gradient.
(2) The step size between two subsequent radial points has to be chosen smaller than the typical size of structures in the density distribution in a particular distance r from the star in order to prevent skipping of local density enhancements, etc. (for the simulation of the spectral energy distribution a linear increase/decrease of the density between two subsequent radial points is assumed).

Further Remarks:

- The quantity $n(r)$ represents the *relative* number of grains. The absolute number of grains is estimated internally based on the total mass of the dust configuration, specific dust density and grain size distribution.
- A radial grid with a logarithmic equidistant distribution of grid points is a good choice in case of "smooth" density distribution decreasing towards the radiative source. In case of a clumpy structure, however, the grid has to be adapted to the size of the clumps in the (radial) regions where they are present. The same applies if for instance circumstellar disks with gaps (due to planet-disk interaction) are considered.
- If the dust density distribution results from an n-particle simulation, one should subdivide the model space in spherical shells centered on the star, estimate the mean relative number density of dust grains in each shell (total number of grains N_i / volume of the shell V_i). Let $n(r_1)$ and $n(r_{100})$ be the number densities at the innermost and outermost shell of a model subdivided into 100 shells. Let r_1 and r_{100} be the corresponding mean radii of these shells. Then, the file prepared for upload of the density distribution might have the following structure (see also Fig. A.2):

# Header with remarks etc. (optional)	
102	
Inner radius	$n(r_1)$
r_1	$n(r_1)$
r_2	$n(r_2)$
...	...
r_{99}	$n(r_{99})$
r_{100}	$n(r_{100})$
Outer radius	$n(r_{100})$

Table A.2
Example upload-file for density distributions resulting from n-particle simulations (see also Fig. A.2).

A.3 Dust Data

A dust species of a particular chemical composition is defined by its specific (material) density, its sublimation radius, and its wavelength-dependent complex refractive index. A large database of laboratory measurements of astrophysically relevant refractive indices is available at
`http://www.astro.uni-jena.de/Laboratory/Database/odata.html`
(Henning et al. 1999).

The file structure for dust data is identical to those accessible through the DDS (see there for examples). It is documented in Tab. A.3.

A.4 Observed SED

The DDS allows to upload observed SEDs in order to overlay them to the results of the simulation. The file structure for observed SEDs is identical to those created by the DDS in order to allow an upload and overlay of simulated SEDs as well (see Sect. B.1). It is documented at *http://aida28.mpia-hd.mpg.de/~swolf/dds/dds-manual.html#obs_sed*.

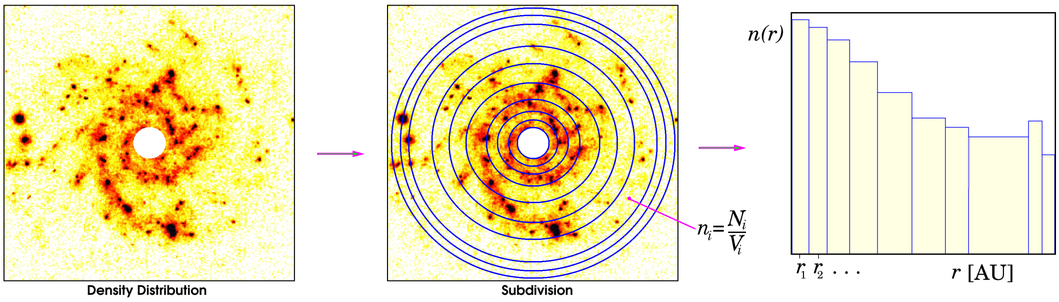

Fig. A.1. Illustration of the subdivision of the model space in case of density distributions resulting from n-particle simulations. The better the radial density distribution is sampled - especially in regions with high density gradients - the higher is the accuracy of the corresponding SED calculated with the DDS (see Sect. A.2).

# Header with remarks etc. (optional) # …		
Identifier (e.g. chemical composition) *[string]*		
Specific dust grain density in units of [g/cm^3] *[integer]*		
Sublimation temperature of the dust grains in units of [K] *[float]*		
Number of Wavelengths in the file *[integer]*		
Wavelength [μm] *[float]* …	Re(refractive index) *[float]* …	Im(refractive index) *[float]* …

Table A.3
File structure required for dust data upload-files.

B Output formats of selected files

B.1 Resulting SED

The file structure for observed SEDs is identical to those created by the DDS (in order to allow an upload of simulated SEDs as well) It is documented in Tab. B.1.

B.2 Radial temperature distribution

The structure of the file with the radial temperature distribution is given in Tab. B.2. For a dust ensemble consisting of grains with different sizes and

# Header # containing a description of the model			
Wavelength [μm] *[float]*	Flux [mJy] *[float]*	0.0	0.0
...	...	...	...

Table B.1
Structure of the output file with the calculated SED.

# Header	
Radial distance to the source r [AU] *[float]*	Temperature [K] *[float]*
...	...

Table B.2
Structure of the output file with the radial temperature distribution.

chemical composition, the radial temperature profile is stored for each single grain species. Following algorithm to write out the data is implemented:

```
for all chemical compositions
   for all grain sizes
       write brief header containing the current
         chemical composition and grain size
         (starting with a "#" sign)
       for r_sub ≤ r ≤ outer radius
          write r, T(r)
       end for
   end for
end for
```

References

[1] Dermott, S.F., Durda, D.D., Gustafson, B.A., Jayaraman, S., Xu, Y.L., Gomes, R.S., Nicholson, P.D. 1992, in Asteroids, Comets, Meteors, A.W. Harris & E. Bowell (eds.), 153

[2] Dorschner, J., Begemann, B., Henning, Th., Jäger, C., Mutschke, H. 1995, A&A, 300, 503

[3] Greaves, J.S., Holland, W.S., Moriarty-Schieven, et al. 1998, ApJ, 506, L133

[4] Henning, Th., Il'In, V.B., Krivova, N.A., Michel, B., Voshchinnikov, N.V. 1999, A&AS, 136, 405

[5] Holland, W.S., Greaves, J.S., Zuckerman, B., et al. 1998, Nature, 392, 788

[6] Jäger, C., Mutschke, H., Henning, Th. 1998, A&A, 332, 291

[7] Kalas, P., Jewitt, D. 1995, ApJ, 110, 794

[8] Liou, J.-C., Dermott, S.F., Xu, Y.-L. 1995, Planet. Space Sci., 43, 717

[9] Meyer, M.R. 2001, AAS, 198, #25.06

[10] Voshchinnikov N.V. 2004, Astrophys. Space Phys. Rev., 12, 1

[11] Weinberger, A.J., Becklin, E.E., Zuckerman, B. 2003, ApJ, 584, L33

[13] Wolf, S. 2003 Comp. Phys. Comm., 150, 99

[13] Wolf, S., Voshchinnikov, N.V. 2004, Comp. Phys. Comm., in press